Nuclear matter EOS in the leading order Brueckner theory with the three-nucleon interaction from chiral EFT

M. Kohno, Research Center for Nuclear Physics, Osaka, Japan

- LOBT calculations of the nuclear matter saturation curve, using NN and 3N interactions in chiral effective field theory (Ch-EFT).
  - Role of the 3NF to reproduce correct saturation properties, and a physical picture behind.
- Results for neutron matter.
- Hyperon properties in nuclear matter: implication of the present NLO YN interactions by the Bonn-Julich group.
  - Possible contributions from the NLO ΛNN force.

Salient features of atomic nuclei

- Atomic nuclei: basic components in our ordinary hadronic world, in the intermediate-period between the big-bang and black-holes or neutron stars.
- Salient features of nuclei: fundamental for various quantum mechanical phenomena of nuclei.
  - Saturation
  - Shell-structure (single-particle aspect)
- The basic problem is how to understand these properties on the basis of underlying NN interactions and/or QCD.
- Quantitative understanding is not complete: e.g., discussions about EoS, E_{sym}, slope parameter L, and so on are still ongoing.

Saturation and shell-structure

- Saturation
  - inner densities of nuclei and B.E./A are almost constant from light to heavy nuclei: infinite matter limit, $\rho_0 = 0.17$ fm-3 and B.E./A= 16 MeV
    - a liquid-drop model was thought in the early stage.
- Shell-structure
  - Experiments established single-particle aspects of nuclei, in spite of singularly repulsive NN interactions.
- Bruckner theory in the 1950's paved the way for a (semi-) quantitative explanation.
- Recent progresses:
  - developments of the description of NN and 3N interactions on the basis of chiral symmetry of QCD and effective interaction theory such as $V_{low\ k}$ and SRG.
  - advances of quantum many-body calculations, theoretically and computationally: CCM, GFMC, NCSM, ・・・

How the saturation and s.-p. structure of nuclei appear,
in spite of the NN interaction singular at short distance?

- Brueckner theory (1950s) provided a semi-quantitative explanation.
  - The "effective" interaction namely G-matrix, after short-range correlations are taken into account by the matrix equation $\boldsymbol{G(\omega) = v + v\frac{Q}{\omega - H}G(\omega)}$, is weak enough to produce mean field.
    - Importance of the Pauli and dispersion effects.
    - Saturation mechanism: the attraction from the tensor correlation becomes weaker at larger densities due to the Pauli blocking.
- However, no realistic NN potential with high accuracy can reproduce correct saturation properties in nuclear matter. (Energies and radii of nuclei are not simultaneously reproduced in *ab initio* calculations.)

Understanding nuclear saturation properties

- Microscopic studies based on bare NN forces
  - Brueckner theory (1950's , LOBT)
- Standard explanation
  - Strong short-range repulsion
  - Pauli effects suppress tensor correlations.

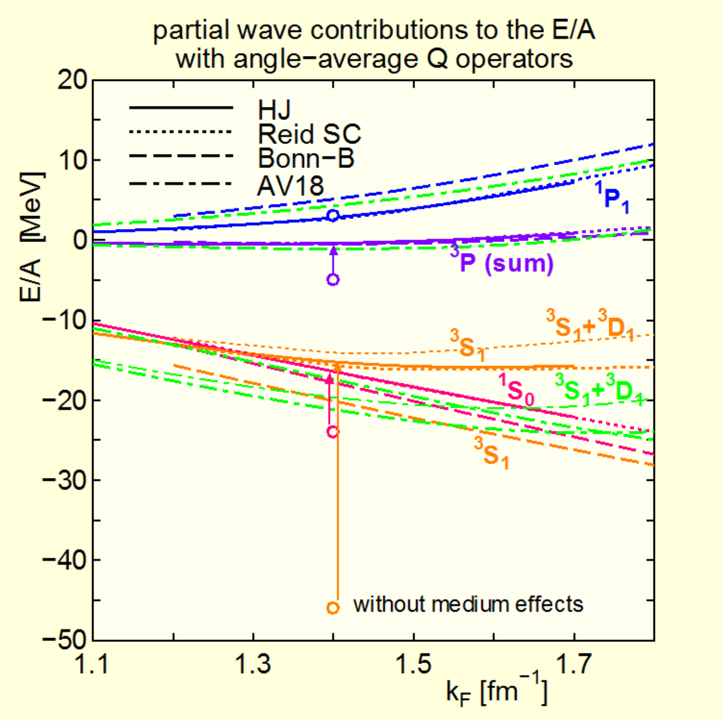

- Quantitative insufficient.
  - Saturation point is located at higher densities.

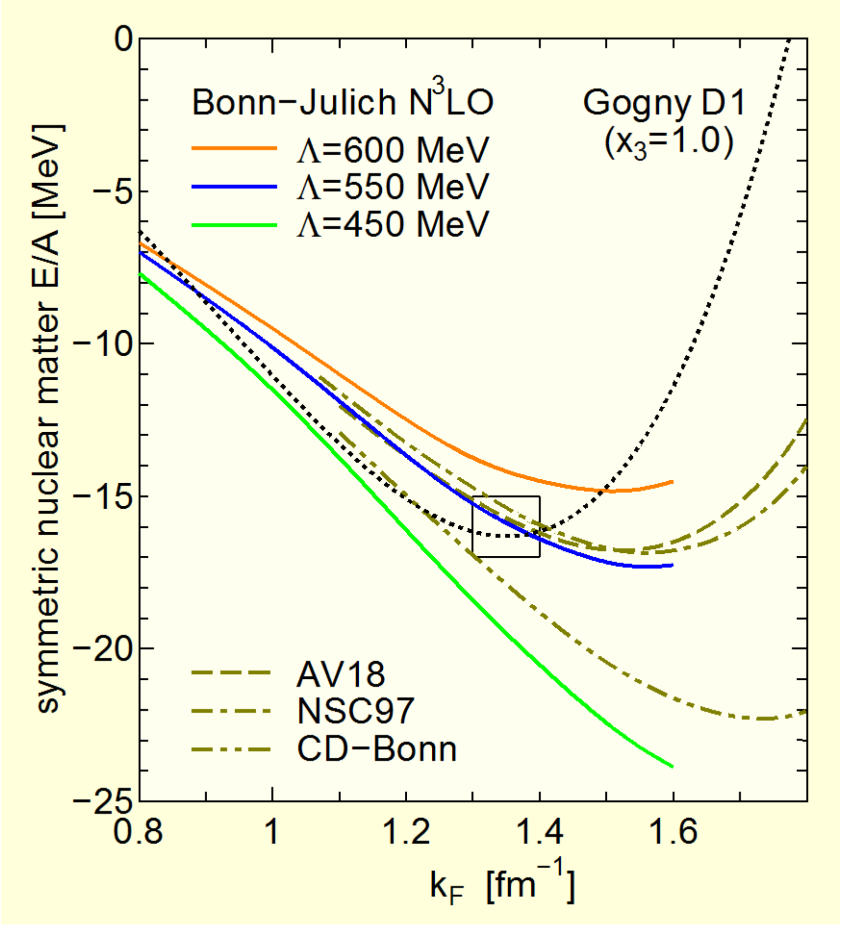

Equivalent interaction in restricted (low-mom.) space

$\langle k'|H|k\rangle$ $\widetilde{H} = e^{-S_{12}}He^{S_{12}}$ $\langle k'|\widetilde{H}|k\rangle$

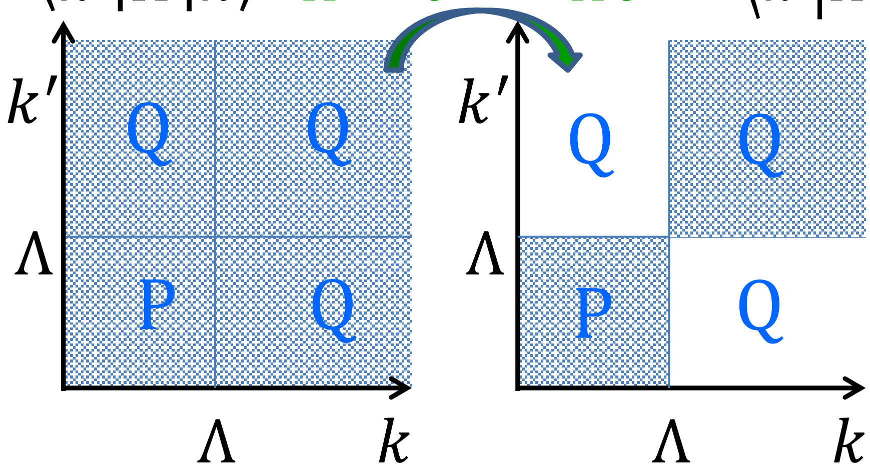

- Apply a unitary transformation $e^{S_{12}}$ to H to obtain an equivalent Hamiltonian $\widetilde{H}$ in a restricted (P) space

  [Suzuki and Lee, PTP64 (1980)]

- The unitary tf. $e^{S_{12}}$ should satisfy a decoupling condition $\langle Q|\widetilde{H}|P\rangle = \langle P|\widetilde{H}|Q\rangle = 0$ in two-body space (block-diagonal).
  - Singular high-momentum components are eliminated.
- Eigenvalues, namely on-shell properties, in the restricted (P) space do not change.
  - Off-shell properties naturally change.
- Induced many-body forces appear in many-body space.

Nuclear matter saturation curves with various modern NN forces

- LOBT calculations do not reproduce the empirical saturation point.
  (Higher order contributions are believed to be small.)
- Off-shell uncertainties: Coester band [F. Coester et al., Phys. Rev. C1, 769 (1970)]

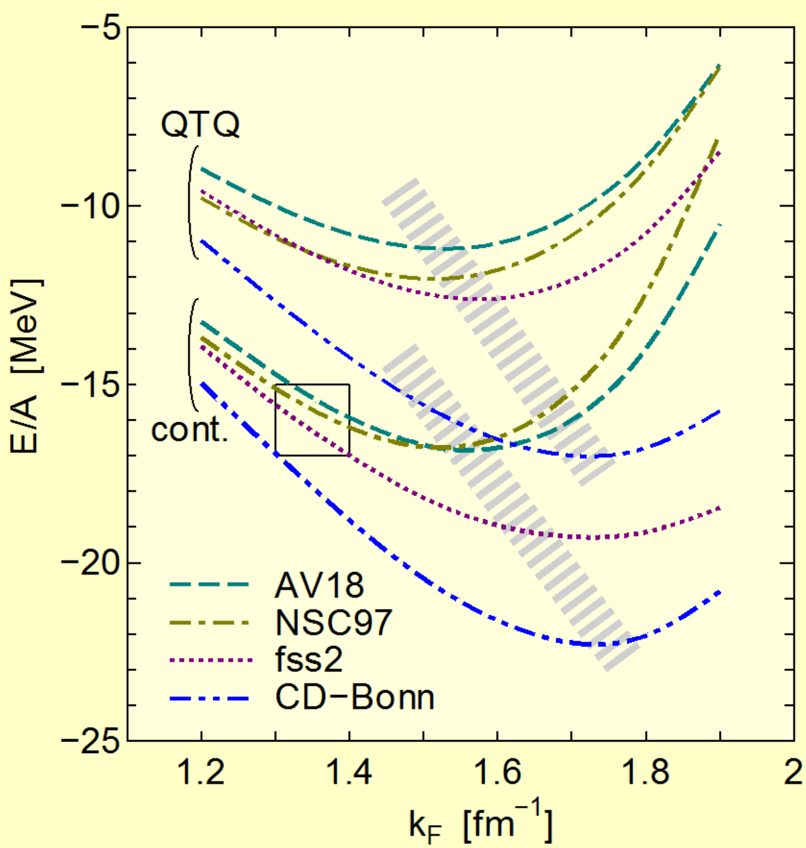

[various modern realistic NN potentials]

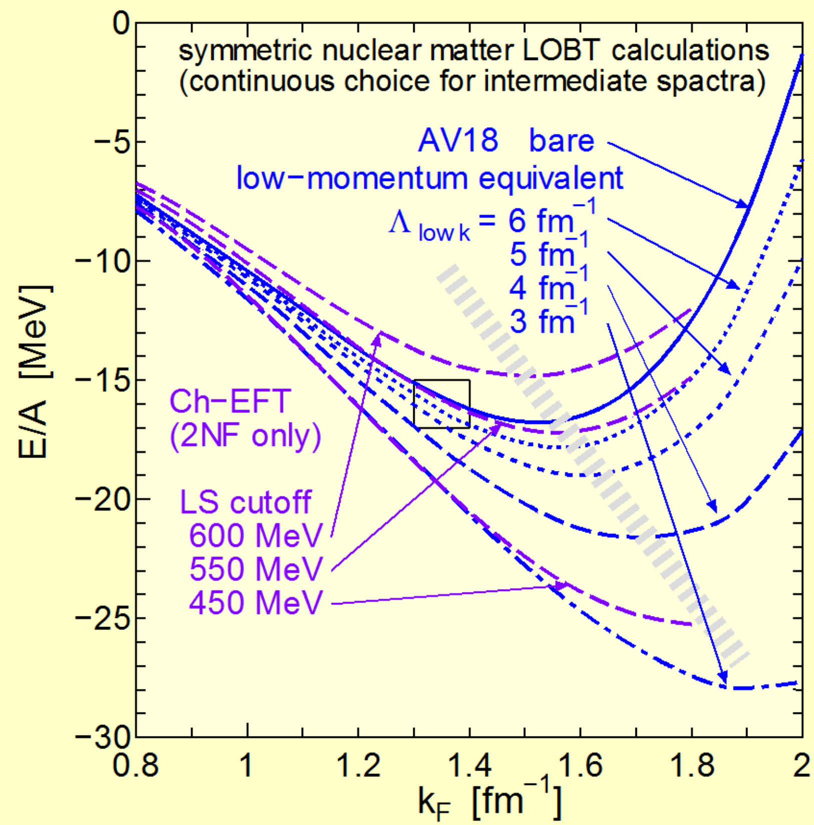

[low momentum interactions from AV18, and Ch-EFT with three choices of cutoff scale Λ]

Nuclear matter saturation curves with various modern NN forces

- LOBT calculations do not reproduce the empirical saturation point.
  (Higher order contributions are believed to be small.)
- Off-shell uncertainties: Coester band [F. Coester et al., Phys. Rev. C1, 769 (1970)]

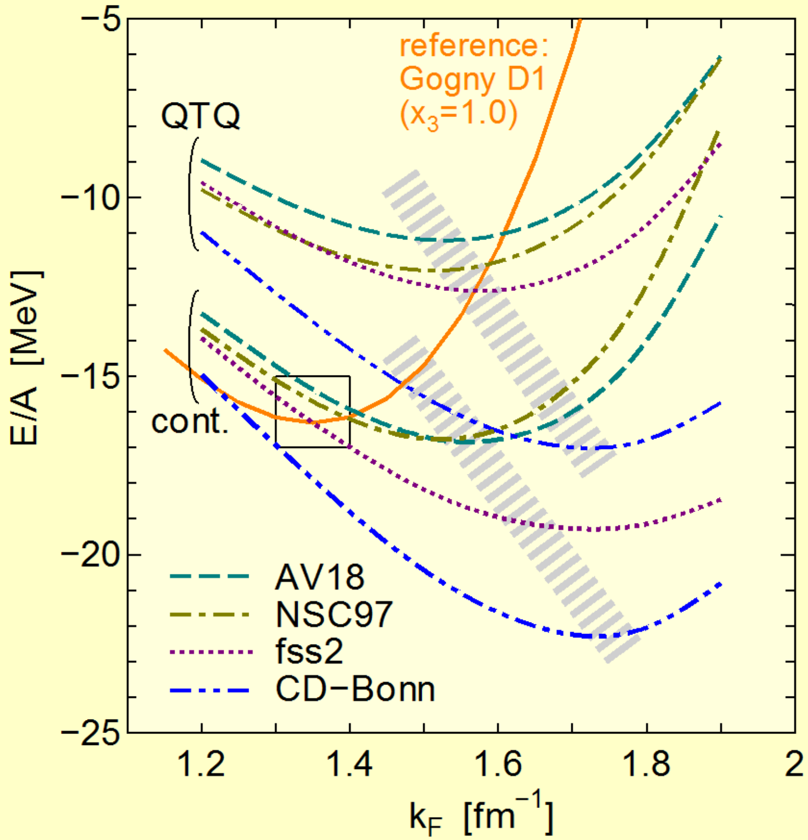

[various modern realistic NN potentials]

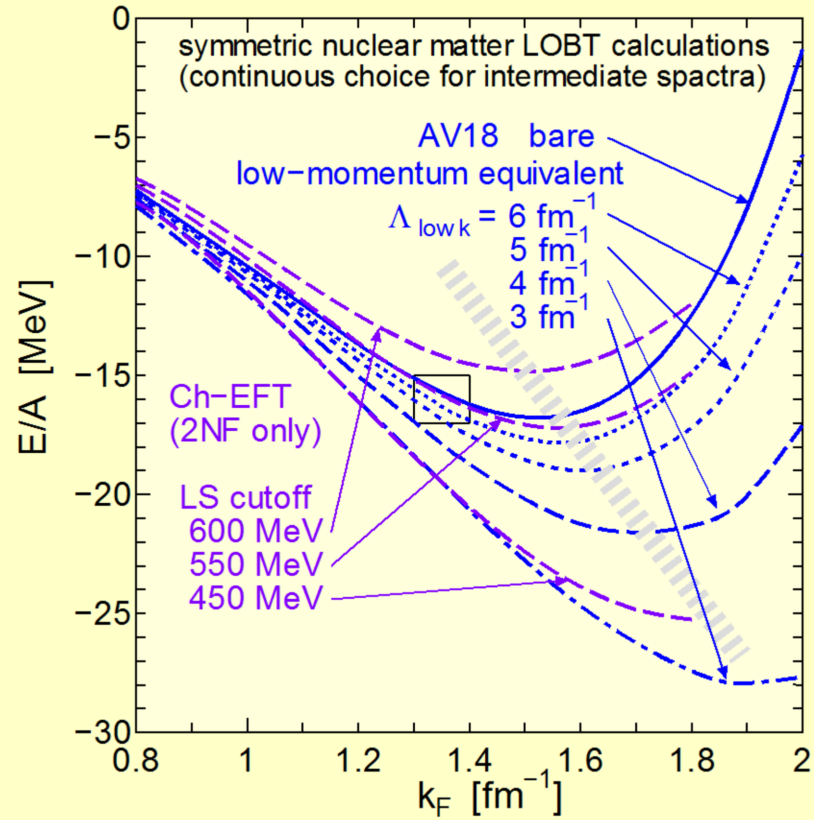

[low momentum interactions from AV18, and Ch-EFT with three choices of cutoff scale Λ]

Missing effects or contributions?

- Possible effects to be taken care of:
  - Higher orders, relativistic effects, 3NF, medium modification, ...
- Since the 1950s, 3NF effects have been expected.
  - It has been known that the Δ-excitation, which provides attraction in the $^1S_0$ channel in free space, is Pauli-blocked in the medium.
  - This effect can be understood as the contribution of the Fujita-Miyazawa 3NFs.

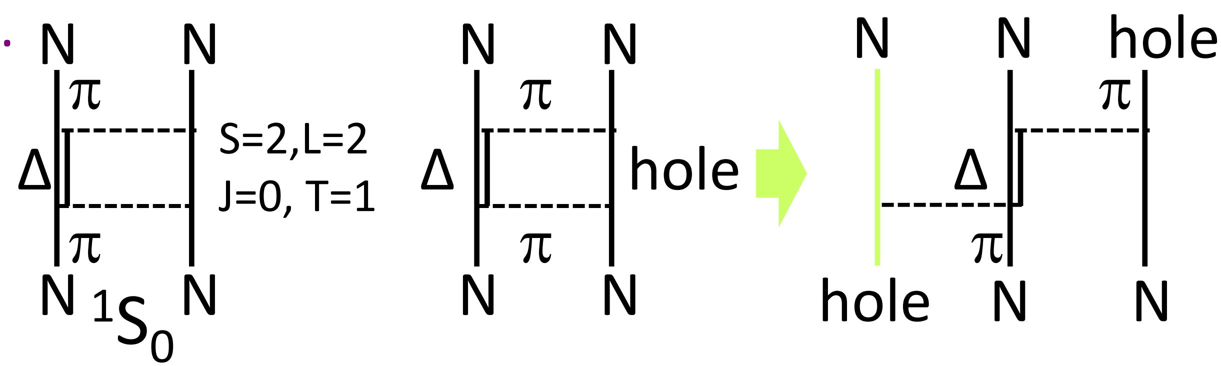

- Phenomenological terms and adjustments were included in all studies of 3NF effects in the literature.
  - Variational calculations by Pandharipande *et al*. (1980-2000)

NN interaction in chiral-effective field theory

- Progress in the description of NN interaction: Ch-EFT
  - At N^{3}LO level, comparable accuracy for reproducing NN scattering data with other modern NN interactions is achieved.
  - 3NFs are introduced (defined) systematically and consistently with the NN sector.
- These 3NFs can, as shown later, reproduce quantitatively saturation properties.

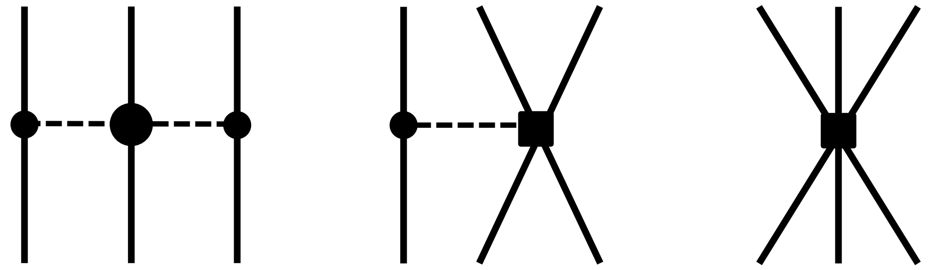

  - 2π-exchange is a lower-energy process to be considered before including anti-nucleons, for example.

Brief introduction of baryon-baryon interactions in Ch-EFT

- Low energy effective theory: starting from a general Lagrangian, which satisfies chiral symmetry of QCD, for low-energy elements of nucleons and pions (a Goldstone boson of the symmetry breaking), NN potential is perturbatively constructed in power counting scheme, by calculating, e.g., Feynman diagrams.

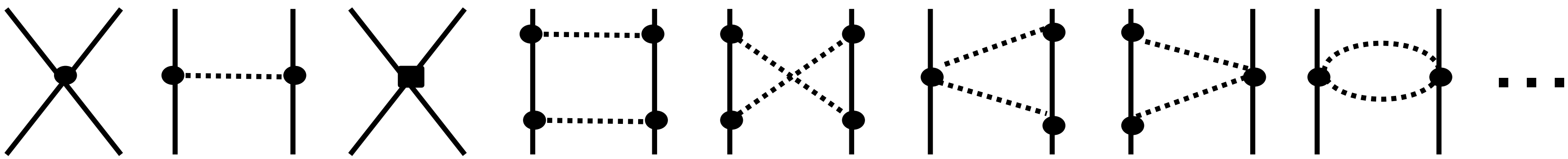

(π, K, η exchange in the case of SU(3))

- Coupling constants are determined by πN and NN data.
  - NN scattering and bound states are not treated by perturbation.
    ➡ Lippmann-Schwinger eq.
  - Renormalization for the divergence of Feynman diagrams and regularization of Lippmann-Schwinger equation at the cutoff scale of the order of $\Lambda = 500 - 600$ MeV.

NNLO 3NFs v_{123} in Ch-EFT

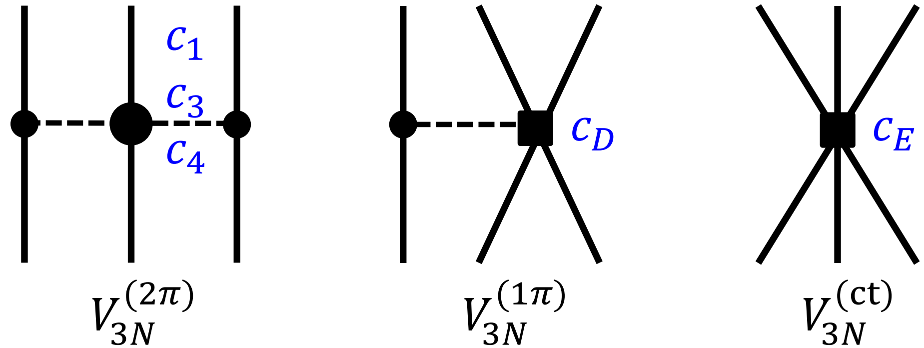

$$V_{123}^{(2\pi)} = \sum_{i\neq j\neq k} \frac{g_A^2}{8f_\pi^4} \frac{(\boldsymbol{\sigma}_i \cdot \boldsymbol{q}_i)(\boldsymbol{\sigma}_j \cdot \boldsymbol{q}_j)}{(\boldsymbol{q}_i^2 + m_\pi^2)(\boldsymbol{q}_j^2 + m_\pi^2)} F_{ijk}^{\alpha\beta} \tau_i^\alpha \tau_j^\beta$$

$$F_{ijk}^{\alpha\beta} = \delta^{\alpha\beta}\left[-4c_1 m_\pi^2 + 2c_3 \boldsymbol{q}_i \cdot \boldsymbol{q}_j\right] + c_4 \epsilon^{\alpha\beta\gamma} \tau_k^\gamma \boldsymbol{\sigma}_k \cdot (\boldsymbol{q}_i \times \boldsymbol{q}_j)$$

$$V_{123}^{(1\pi)} = -\sum_{i\neq j\neq k} \frac{g_A c_D}{8f_\pi^4 \Lambda_\chi} \frac{\boldsymbol{\sigma}_j \cdot \boldsymbol{q}_j}{(\boldsymbol{q}_j^2 + m_\pi^2)} \boldsymbol{\sigma}_i \cdot \boldsymbol{q}_j \boldsymbol{\tau}_i \cdot \boldsymbol{\tau}_j$$

$$V_{123}^{(\mathrm{ct})} = \sum_{i\neq j\neq k} \frac{c_E}{2f_\pi^4 \Lambda_\chi} \boldsymbol{\tau}_i \cdot \boldsymbol{\tau}_j$$

$\boldsymbol{q}_i = \boldsymbol{p}_i - \boldsymbol{p}_i$, $\Lambda_\chi = 700$ MeV

$c_1 = -0.81\ \mathrm{GeV}^{-1}$, $c_3 = -3.4\ \mathrm{GeV}^{-1}$, and $c_4 = 3.4\ \mathrm{GeV}^{-1}$ are fixed in NN sector. c_D and c_E are to be determined in many-body systems.

Reduction of 3NF v_{123} to density dependent NN $v_{12(3)}$

$$\langle ab | v_{12(3)} | cd \rangle_A \equiv \sum_h \langle abh | v_{123} | cdh \rangle_A$$

Diagrammatical representation by Holt *et al*.

[J.W. Holt, N. Kaiser, and W. Weise, Phys. Rev. C81, 024002 (2010)]

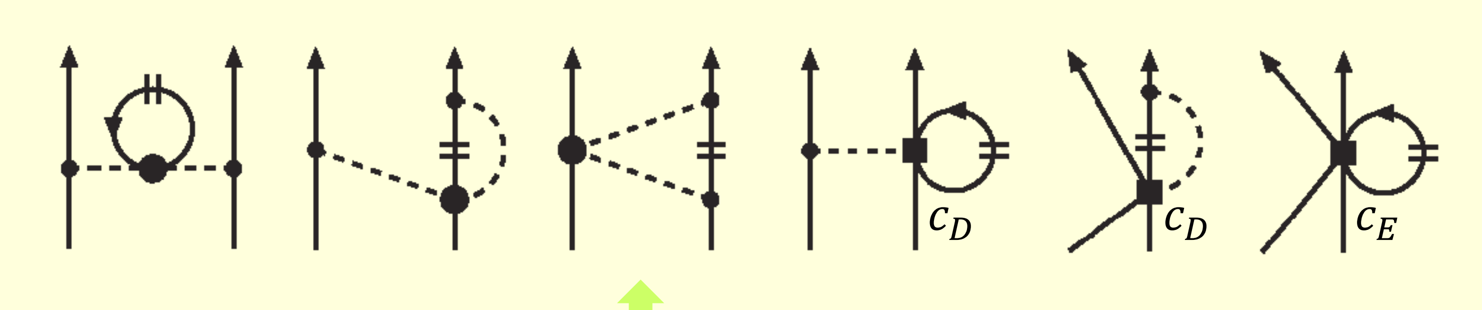

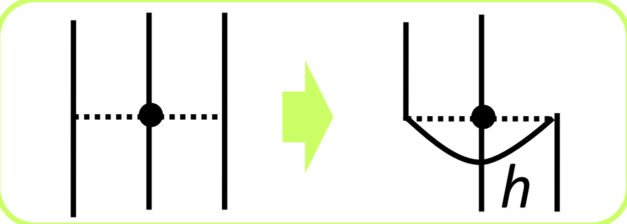

- This diagram partly corresponds to the Pauli blocking of the isobar Δ excitation in a conventional picture.

- Expand them into partial waves, add them to NN and carry out G matrix calculation.
  - A factor of $\frac{1}{3}$ is needed for the calculation of energy.

Statistical factors for 3NF contributions on the HF level

Some caution in evaluating 3NF contributions to the total energy E and s.p. energy e_h.

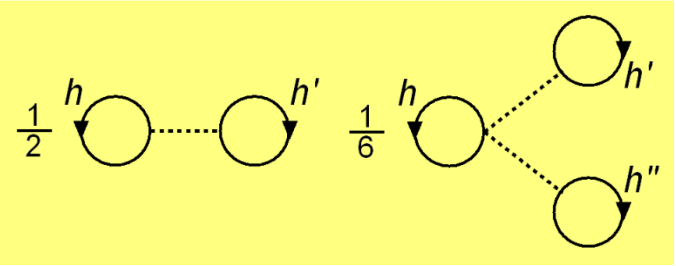

- Total energy (in the HF approximation)

$$E = \sum_h \langle h|t|h\rangle + \frac{1}{2!}\sum_{hh'} \langle hh'|v_{12}|hh'\rangle_A + \frac{1}{3!}\sum_{hh'h''} \langle hh'h''|v_{123}|hh'h''\rangle_A$$

$$\boxed{\text{define } \left\langle ab\middle|v_{12(3)}\middle|cd\right\rangle_A \equiv \sum\nolimits_h \langle abh|v_{123}|cdh\rangle_A}$$

$$= \sum\nolimits_h \langle h|t|h\rangle + \frac{1}{2!}\sum\nolimits_{hh'} \left\langle hh'\middle|v_{12} + \frac{1}{3}v_{12(3)}\middle|hh'\right\rangle_A$$

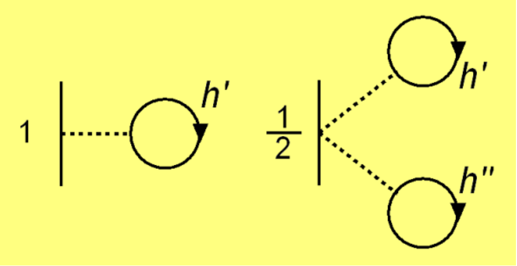

- Single-particle energy (potential)

$$e_h = \langle h|t|h\rangle + \sum\nolimits_{h'} \langle hh'|v_{12}|hh'\rangle_A + \frac{1}{2!}\sum\nolimits_{h'h''} \langle hh'h''|v_{123}|hh'h''\rangle_A$$

$$= \langle h|t|h\rangle + \sum\nolimits_{h'} \left\langle hh'\middle|v_{12} + \frac{1}{2}v_{12(3)}\middle|hh'\right\rangle_A$$

$$= \langle h|t|h\rangle + \sum\nolimits_{h'} \left\langle hh'\middle|v_{12} + \frac{1}{3}v_{12(3)}\middle|hh'\right\rangle_A + \sum\nolimits_{h'} \left\langle hh'\middle|\frac{1}{6}v_{12(3)}\middle|hh'\right\rangle_A$$

Prescription for the G matrix equation including "3NF" term

$$G_{12} = \left(v_{12} + \frac{1}{3}v_{12(3)}\right) + \left(v_{12} + \frac{1}{3}v_{12(3)}\right)\frac{Q}{\omega - H}G_{12}$$

- total energy is given by $E = \sum_k \left\{\langle k|t|k\rangle + \frac{1}{2}U_E(k)\right\}$,

  where $U_E(k) \equiv \sum_{k'}\langle \boldsymbol{k}\boldsymbol{k}'|G_{12}|\boldsymbol{k}\boldsymbol{k}'\rangle_A$
- s.p. energy $e_k = \langle k|t|k\rangle + U_G(k)$, and the potential in the propagator $\omega - H = e_{k_1} + e_{k_2} - (t_1 + U_G(k_1') + t_2 + U_G(k_2'))$
  - The factor in front of $v_{12(3)}$ is different in $U_G(k)$:

    $$U_G(k) \equiv \sum_{k'}\left\langle kk'\middle|G_{12} + \frac{1}{6}v_{12(3)}\left(1 + \frac{Q}{\omega - H}\right)G_{12}\middle|kk'\right\rangle_A$$

    - Note that the difference between $U_E(k)$ and $U_G(k)$ is typically 5 MeV, and this difference does not much affect G, because of the cancellation in the denominator $\omega - H$.
- Note that OMP potential corresponds to $U_G(k)$.

Reducing 3NFs to effective NN interactions in infinite matter

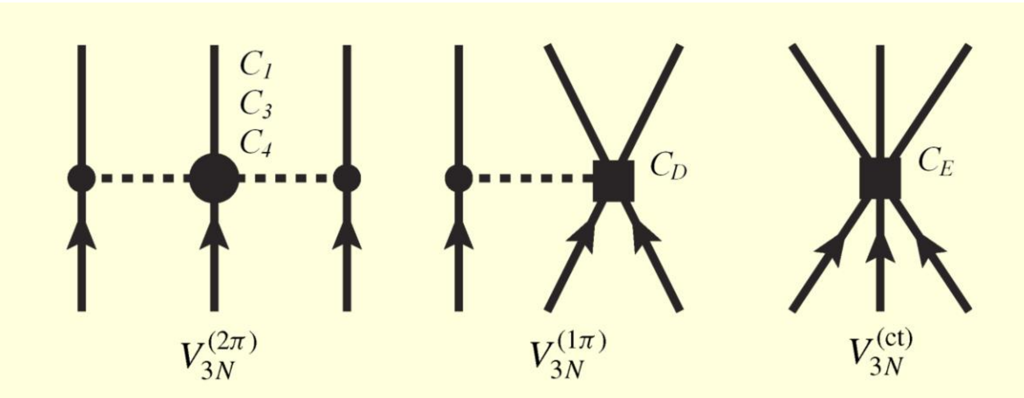

- $c_1, c_3,$ and c_4 are fixed in the NN sector
- c_D and c_E are determined in many-body systems.

- Reduction to effective two-body forces by folding the third nucleon in infinite matter.

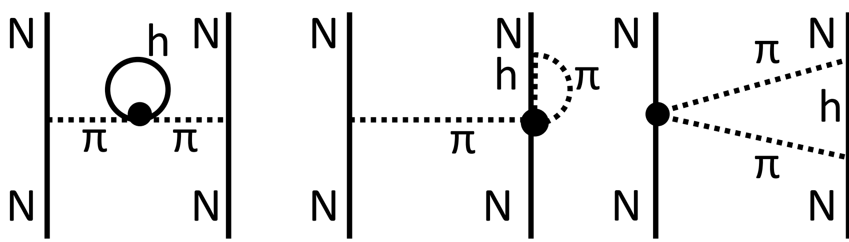

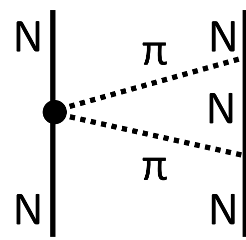

- Contributions of left two-diagrams (wave-function-renormalization and vertex-correction types) tend to cancel.

- In free space:
  - Attractive in $^1S_0$.
  - Suppress 1-π exchange tensor.
- In the medium
  - Reduce attraction in $^1S_0$.
  - Reduce the suppression of tensor force .

LOBT calculations with NN+"3NF" of Ch-EFT

- Calculated saturation curves with three choices of cutoff Λ.
- Results of $c_D = 0$ and $c_E = 0$.
- Pauli effects are sizable.
- Tune c_D and c_E.

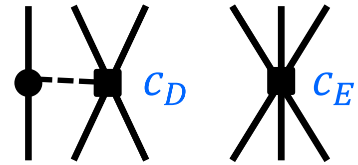

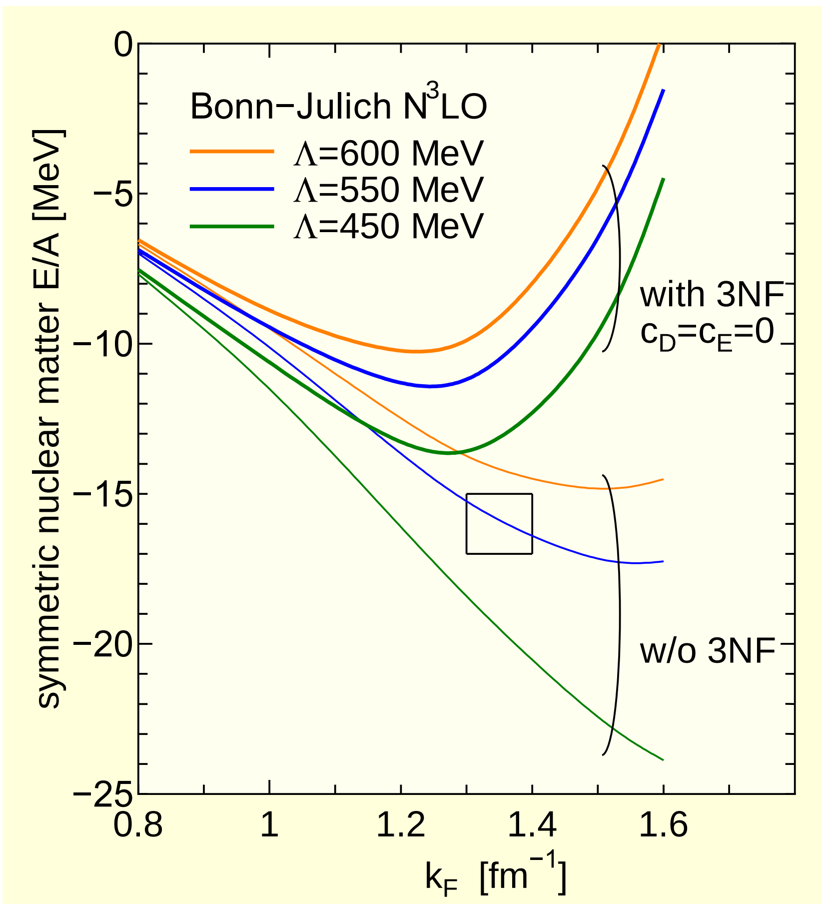

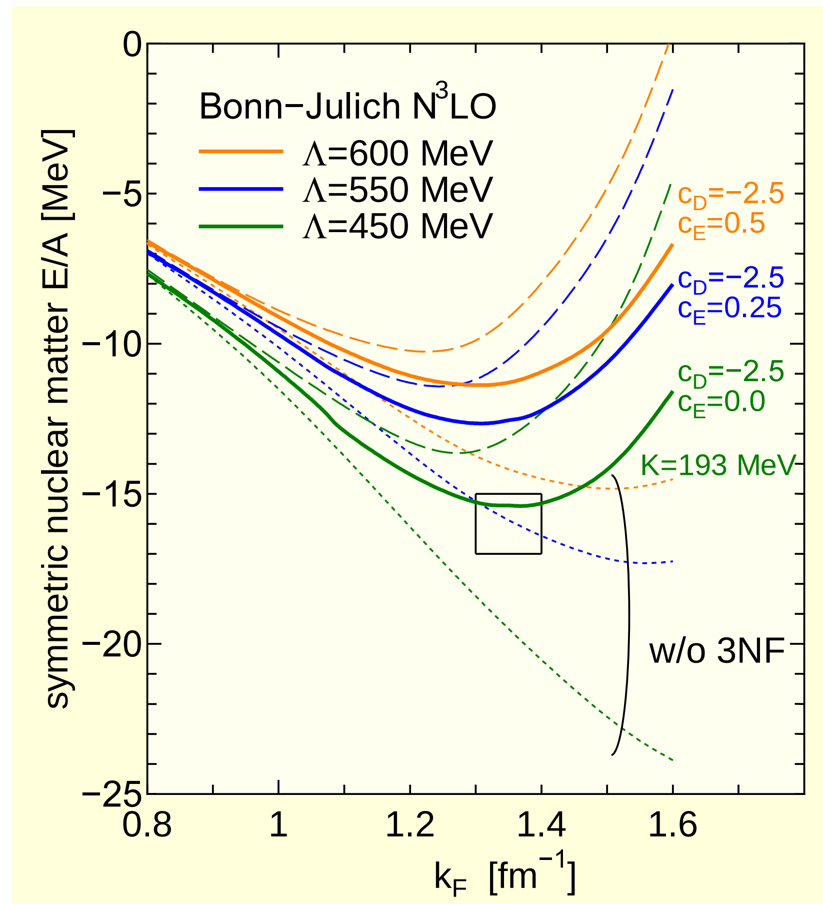

Born energies from the c_D and c_E terms in nuclear matter

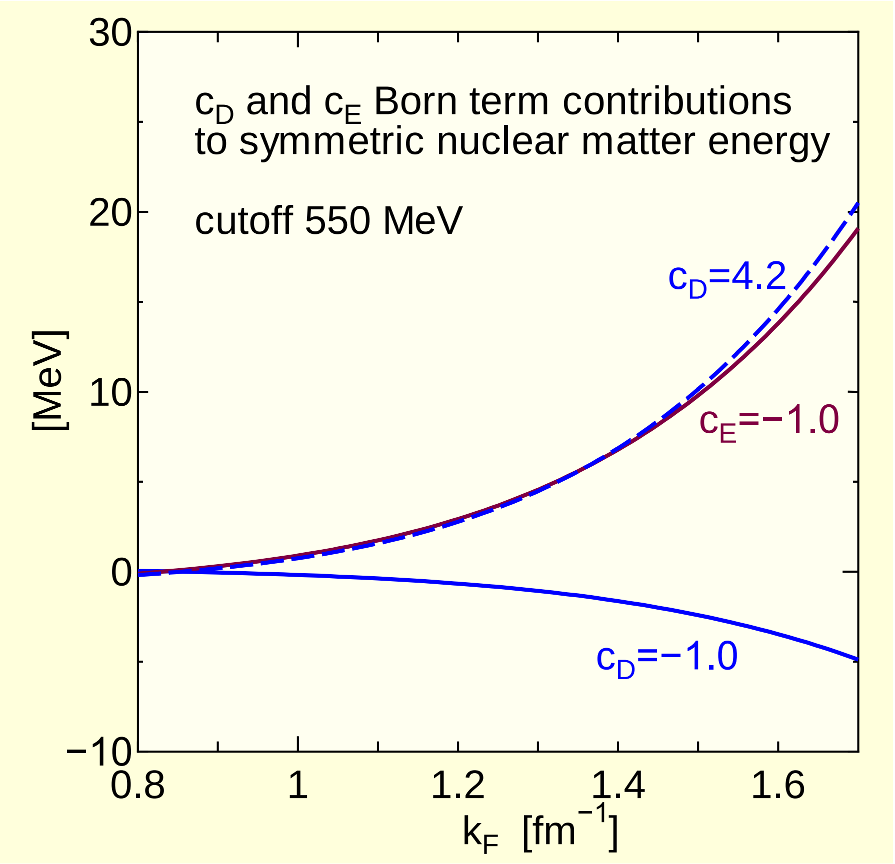

- c_D and c_E terms provide very similar contributions to the nuclear matter HF-level energy, if $c_D \cong -4c_E$.
  - When $c_D \cong 4c_E$ is satisfied, contributions of the c_D and c_E terms cancel.
  - There are continuous uncertainties for c_D and c_E values as far as NM energies are concerned.

Parametrization in the quadratic form of the density ρ:

$$E_{c_D}(\rho) = c_D \times (-0.1902 + 2.952\rho + 37.16\rho^2)$$
$$E_{c_E}(\rho) = c_E \times (0.8695 - 17.52\rho - 128.3\rho^2).$$

each spin- and isospin-channel contribution in LOBT E/A

thin curves : $\Lambda = 450$ MeV,   thick curves: $\Lambda = 550$ MeV

Repulsive contributions of 3NF in ^{3}O and ^{1}S channels.

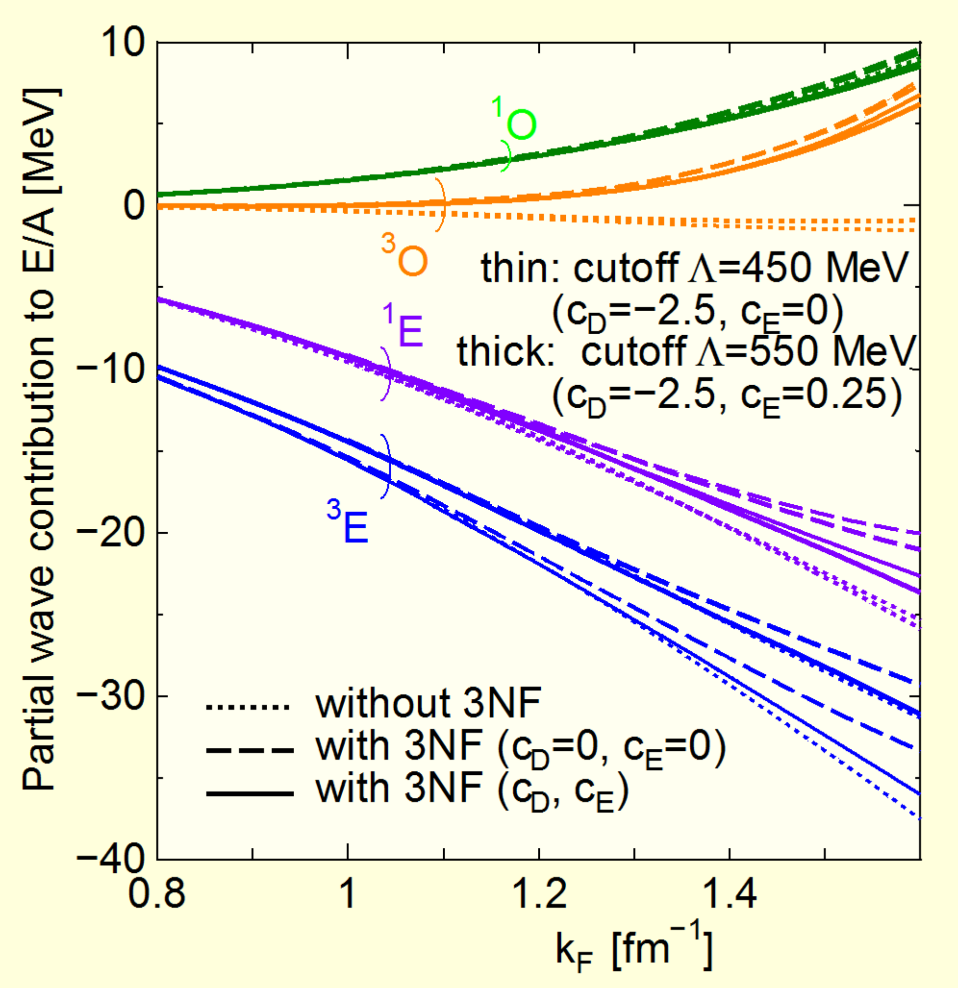

- Repulsive effects of the 3NFs are smaller in ^{3}E state than in ^{1}E state, because of the attraction from the enhanced (∼15%) tensor component.
- Sizable repulsive contribution in ^{3}O state.

Physics behind the repulsive effect in the $^1S_0$ and ^3O states

- It has been known that the Δ-excitation, which produces attraction in the $^1S_0$ state in free space, is Pauli-blocked in the medium.
- This effect can be viewed as the contribution of the Fujita-Miyazawa 3NFs.

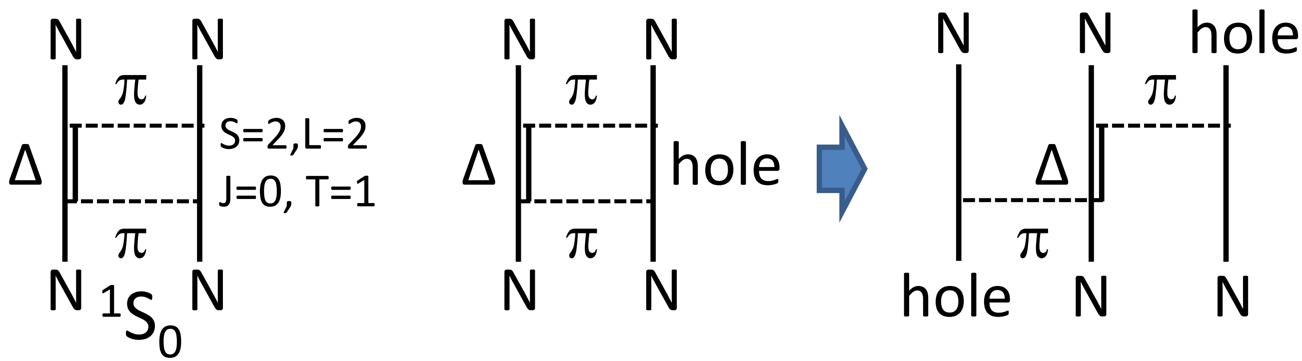

- The corresponding effects appear through a ππNN vertex in Ch-EFT.

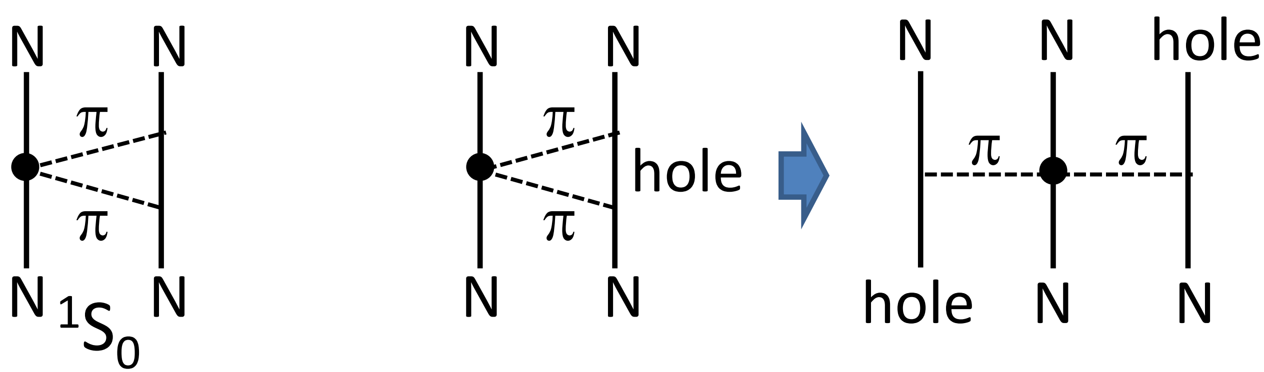

Physics behind the tensor force enhancement in the $^3S_1$ state

- Strong tensor force from one-pion exchange
  - In a OBEP model, ρ-meson exchange provides tensor force in an opposite sign: ➡ natural cut necessary
  - to explain scattering data.

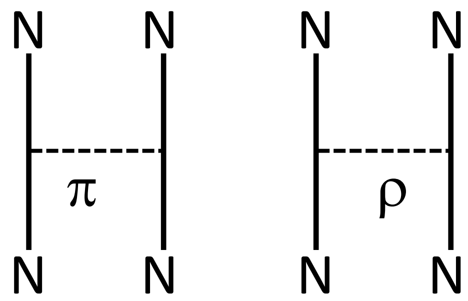

- In Ch-EFT
  - ρ-meson is not present (out of scale).
  - Tensor component from the 2π-exchange plays the role of the ρ-meson. The 2π-exchange is Pauli blocked in the medium, which reduces the suppression of the tensor force:

    ➡ enhancement.

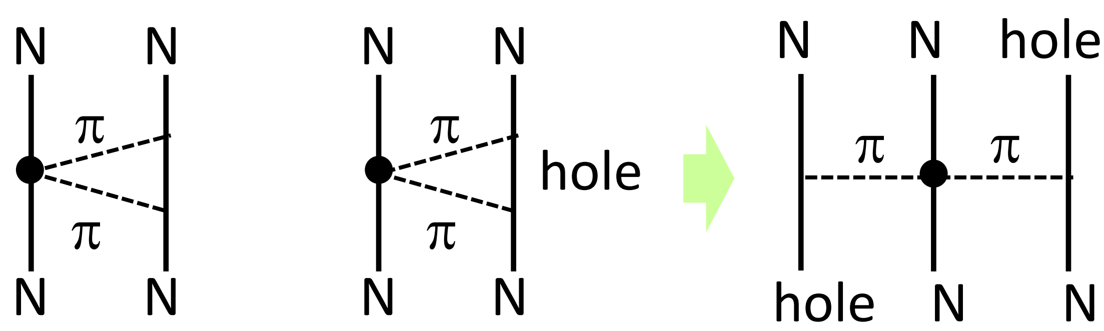

Tensor force including the 3NF effects at normal density

- Bare diagonal matrix elements with and without 3NF effects.
- Diagonal matrix elements of low-momentum tensor interaction.

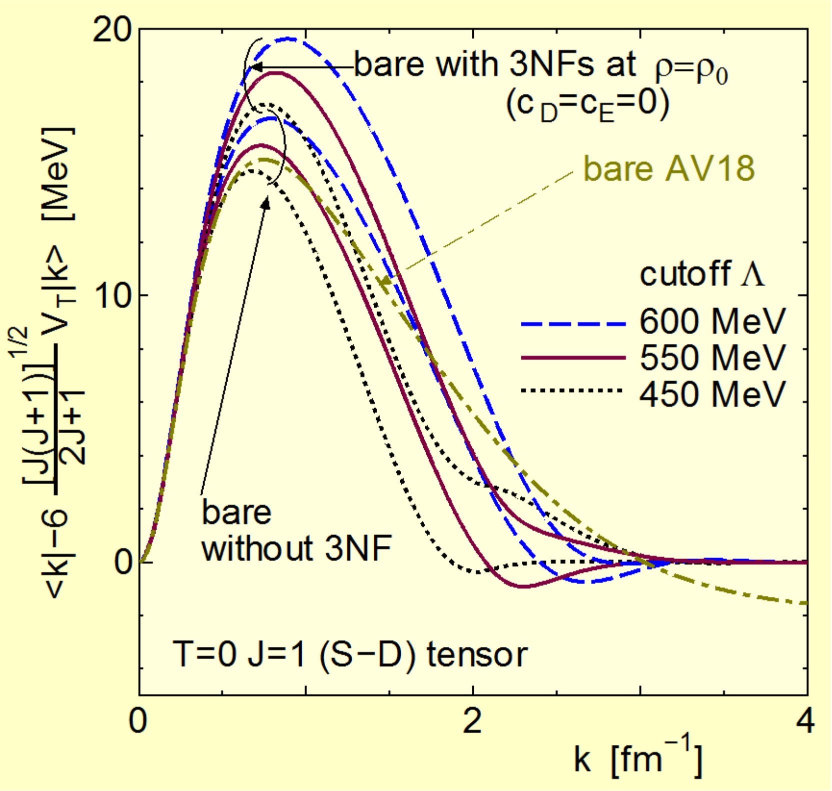

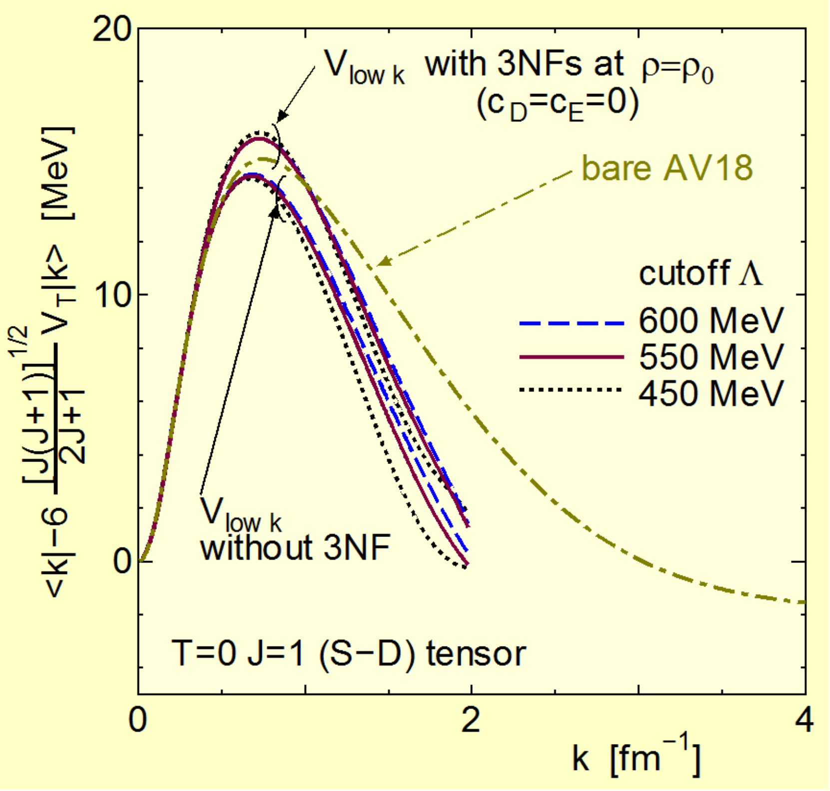

- Tensor force is enhanced by about 15% by the 3NF.
- Cutoff-scale dependence is small in low-momentum space.

Neutron matter

- EoS of neutron matter: basic to theoretical studies of neutron star.
  - EoS of APR, including phenomenological 3NFs, has been standard.
    - Necessity of the repulsive contributions from 3NF.

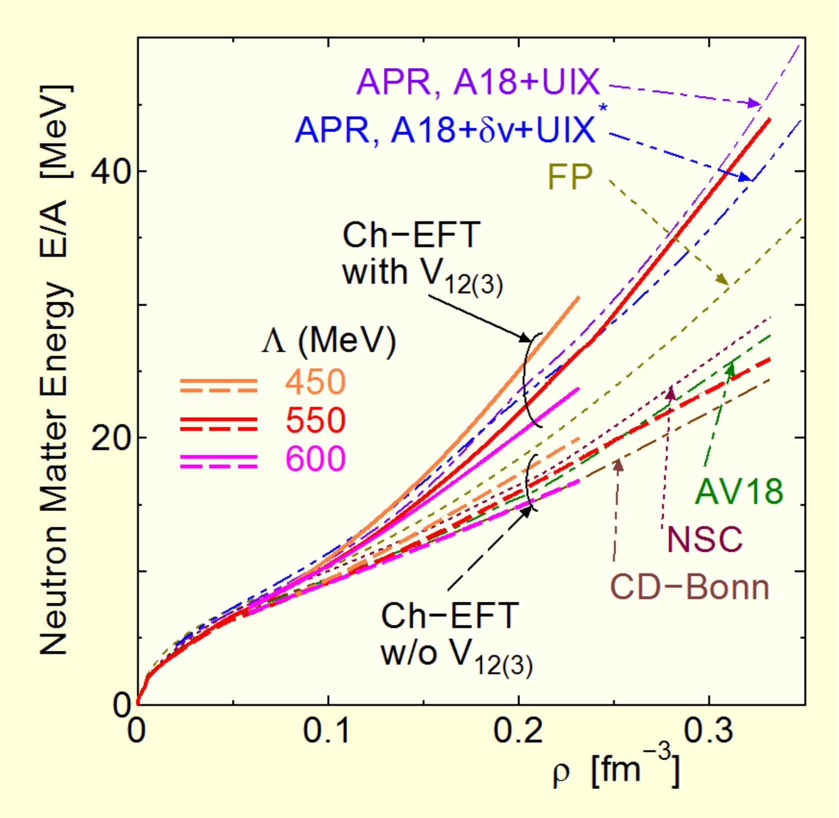

- Dependence on different two-body NN interactions is small, because of the absence of tensor effects in the ^3E state.
- The contribution of Ch-EFT 3NFs (no c_D and c_E terms) is similar to the standard phenomenological one by APR.
  - Ch-EFT is not to be applied to the high-density region of $\rho > 2\rho_0$.

APR: Akmal, Pandharipande, and Ravenhall, PRC58, 1804 (1998)

Neutron matter as a function of ρ/ρ_0

- E/A profile of Gogny D1 force (and some of Skyrme int.) is unrealistic from the point of view of microscopic calculations
  - The density-dependent repulsion is solely taken care of by the ^{3}E state when $x_0 = 1$ in $t_0(1 + x_0 P_\sigma)\rho^\alpha(r_1)\delta(r_1 - r_2)$.

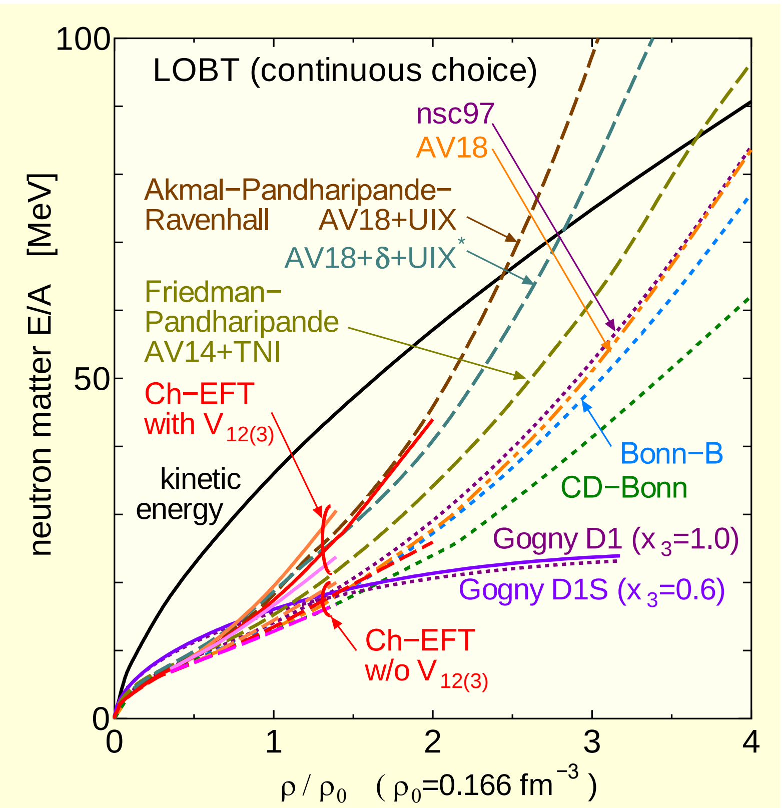

- 3NFs of Ch-EFT imply that repulsion is dominant in ^{1}E and ^{3}O states.

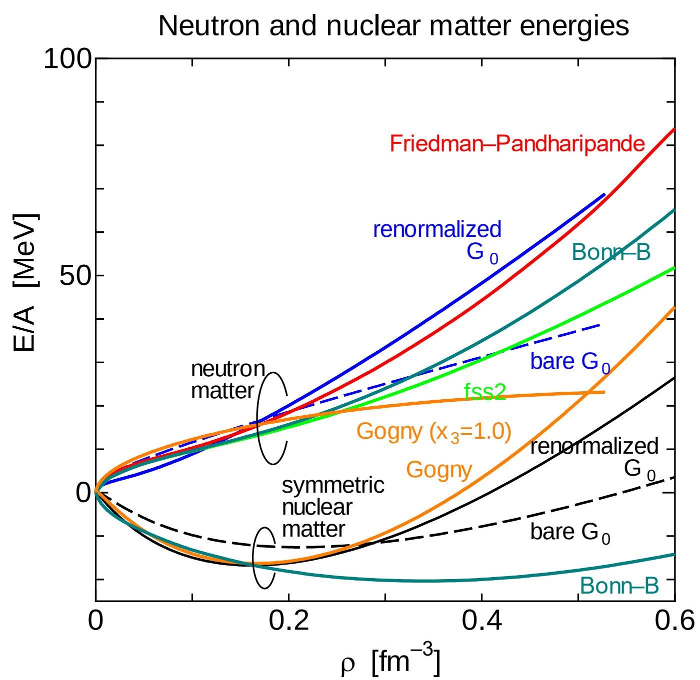

Λ hyperon in neutron matter

- When the s.p. energy of the Λ hyperon becomes smaller than that of the neutron in neutron matter, the Λ hyperon starts to appear through weak processes.

$$m_\Lambda + \frac{\hbar^2}{2m_\Lambda} \times 0^2 + U_\Lambda(0) < m_n + \frac{\hbar^2}{2m_n} \times {k_{F_n}}^2 + U_n\left(k_{F_n}\right)$$

$$U_\Lambda(0) < \frac{\hbar^2}{2m_n} \times {k_{F_n}}^2 - (m_\Lambda - m_n) + U_n\left(k_{F_n}\right)$$

- Calculations in the literature, using realistic NN and YN interactions, indicates that the Λ hyperon should appear at the density of around $3\rho_0$.
- The appearance of the Λ hyperon softens the EoS at high densities.
- Recent observation of $2m_\odot$ neutron stars seems not to support this scenario. Hyperon puzzle.

YN interactions in Ch-EFT

- Parameterization by the Bonn-Julich group
- Lowest order:
  - Polinder et al., Nucl. Phys. A779, 244 (2006)
  - Parameters: $f_{NN\pi} = \frac{2f_\pi}{g_A}$, $\alpha = \frac{F}{F+D}$, and 5 low-energy constants $C^{\Lambda\Lambda}_{1S0}, C^{\Lambda\Lambda}_{3S1}, C^{\Sigma\Sigma}_{1S0}, C^{\Sigma\Sigma}_{3S1}, C^{\Lambda\Sigma}_{3S1}$
- Next-to-Leading order
  - Haidenbauer et al., Nucl. Phys. A915, 24 (2013)
- Leading three-baryon forces
  - Petschauer et al., Phys. Rev. C93, 014001 (2016)

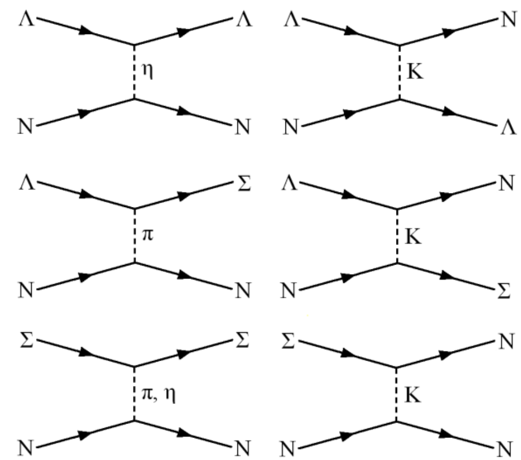

One-pseudoscalar-meson-exchange diagrams
for hyperon-nucleon interactions

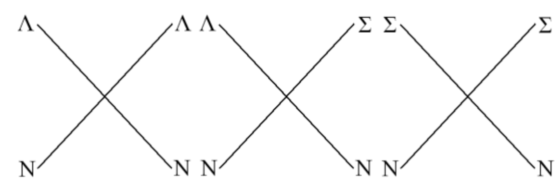

Lowest order contact terms for hyperon-nucleon interactions

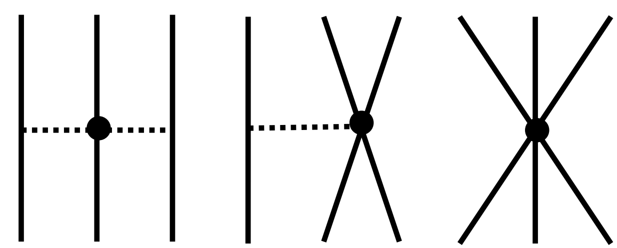

Λ and Σ s.p. potentials in symmetric nuclear matter

- Coupling constants in the NLO level are almost determined by the present YN and hyper-nuclear data.
- The depth of the Λ s.p. potential is shallower than that of other YN potential models.

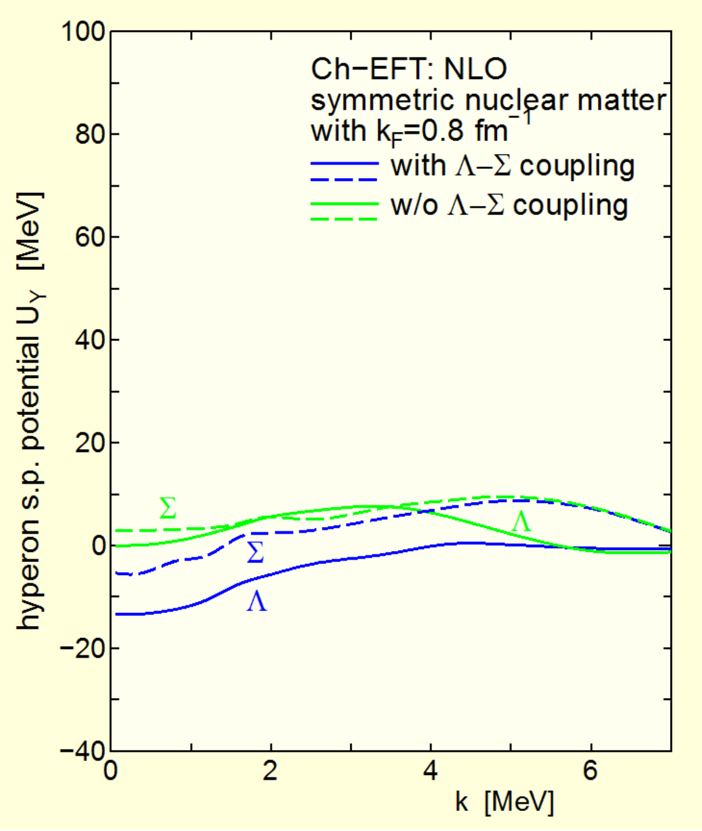

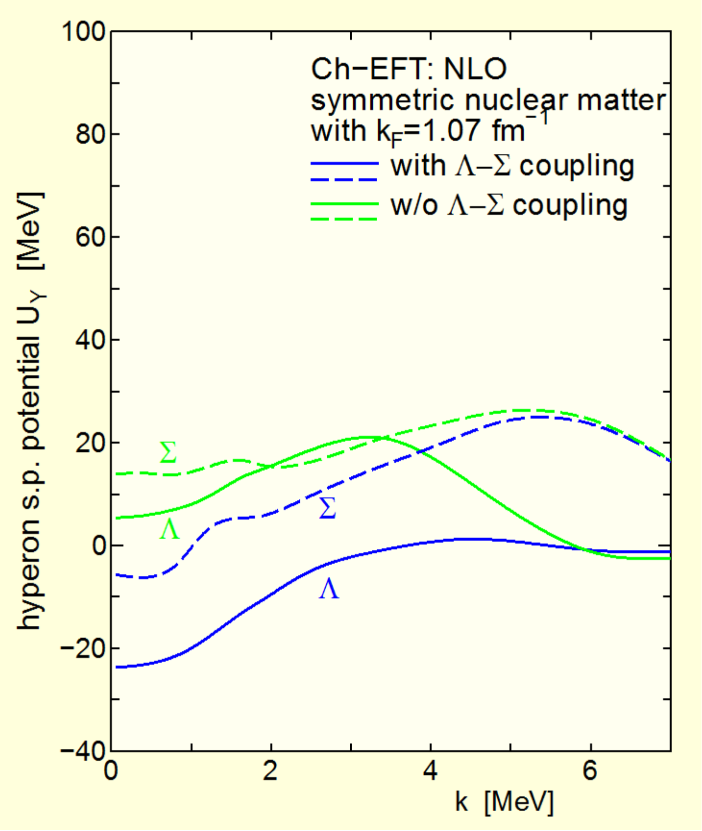

Λ and Σ s.p. potentials in symmetric nuclear matter

- The attraction of the Λ s.p. potential comes from strong ΛN-ΣN coupling.
- The Σ s.p. potential is repulsive.
- The depth of the Λ s.p. potential becomes shallower at higher densities, which has not been seen in other potential models.

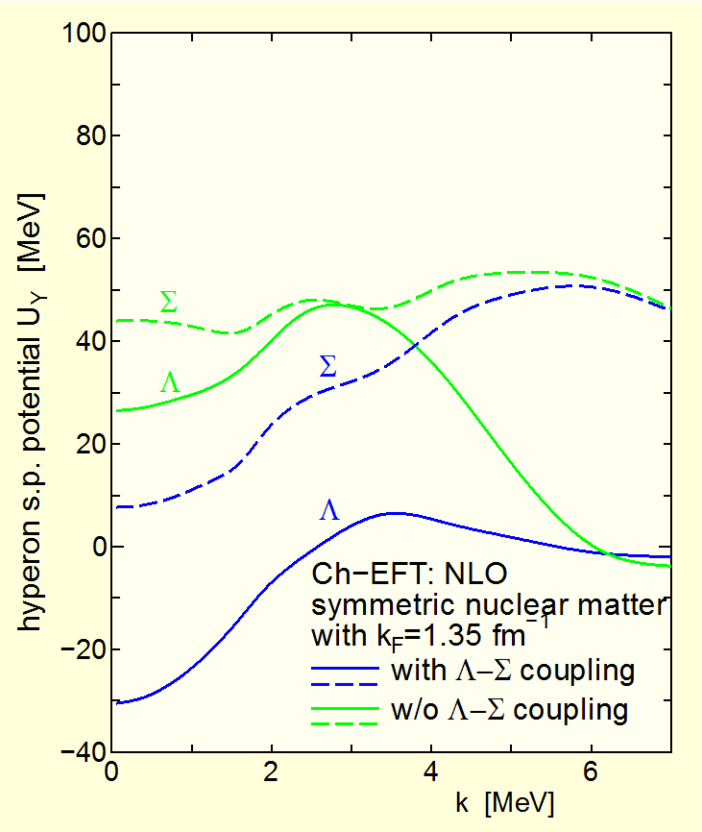

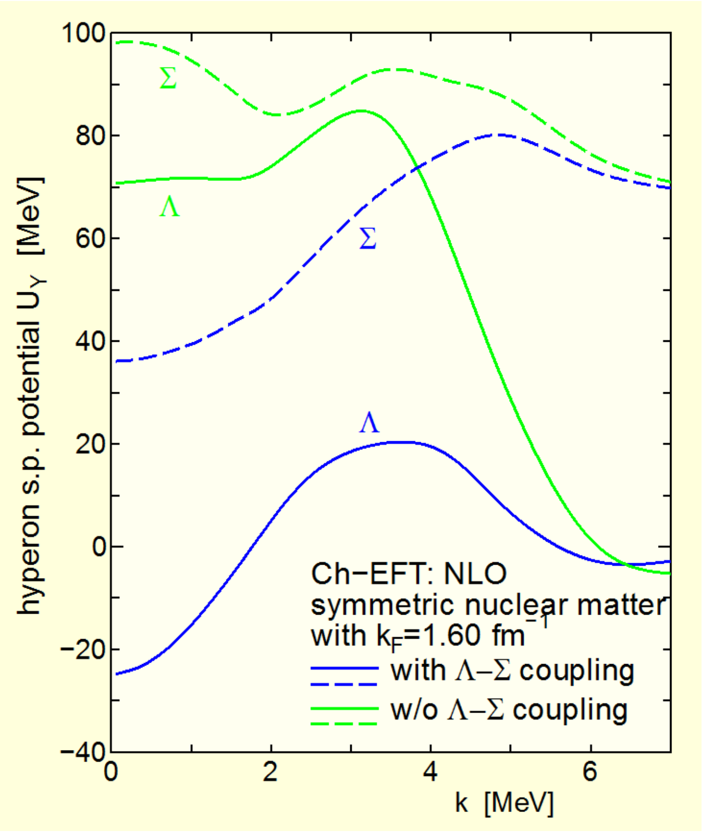

Comparison of the ΛN-ΣN coupling: NSC97 and Ch-EFT

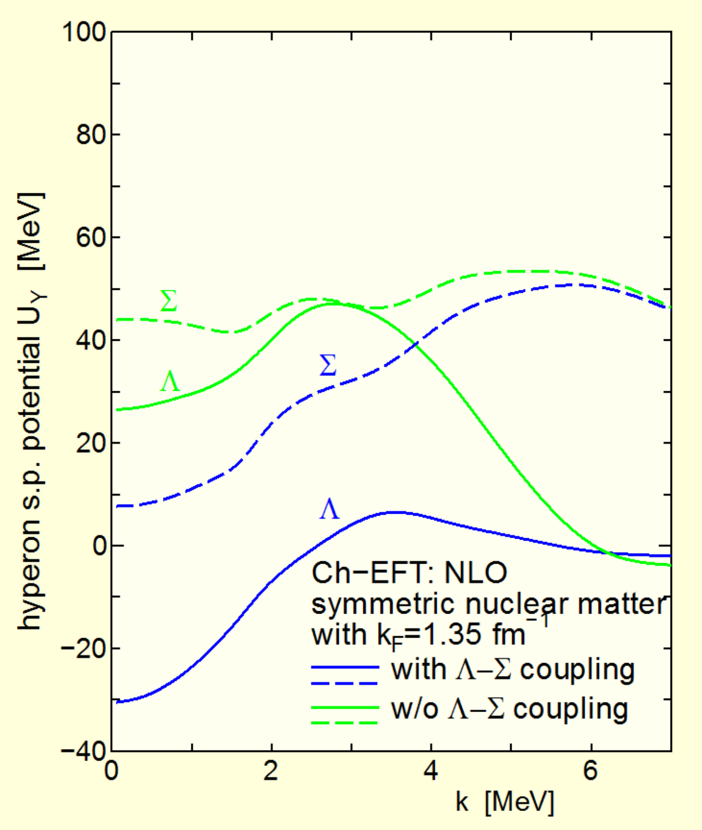

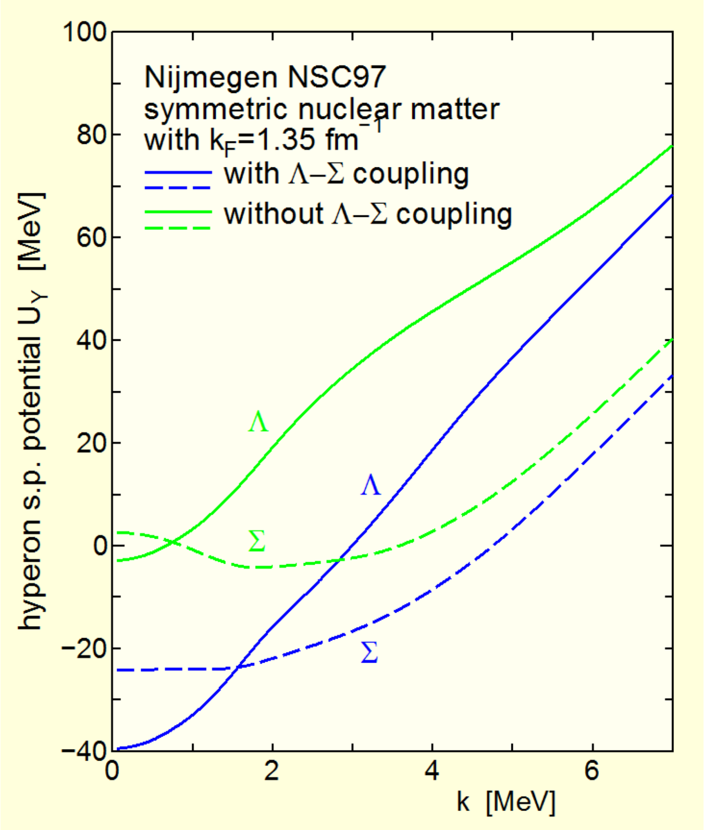

The attraction from the ΛN-ΣN coupling to the Λ s.p. potential is of the order of 60 MeV at the normal density.

Ξ s.p. potential in symmetric nuclear matter

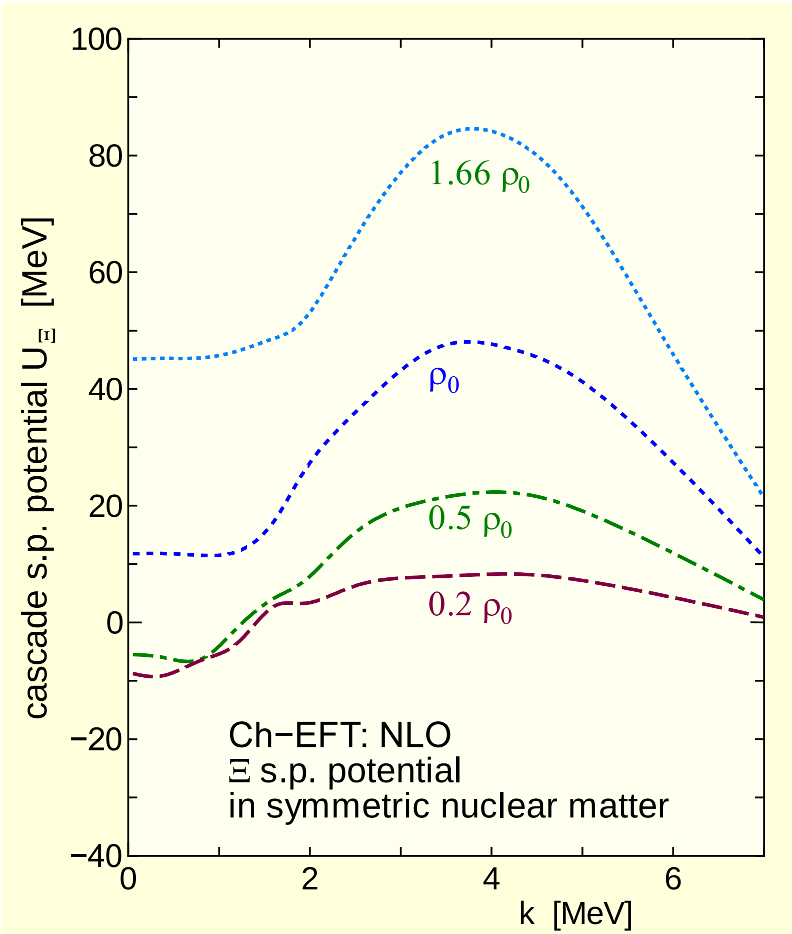

- Large uncertainties for coupling constants in the $S = -2$ sector.
  - One constraint: absence of the H particle state.
- Several-baryon-channels coupling（ΞN-ΛΛ-ΣΣ (T=0), ΞN-ΛΣ-ΣΣ (T=1)）leads to strong state dependence and density dependence.
- Scarce of experimental data.
- Recent experimental progresses:
  - Kiso event: Ξ^{-}-^{14}N (Nakazawa)
  - Ξ bound state in the ^{12}C(K^-,K^+)X reaction at 1.8 GeV/c (Nagae)

3 baryon interaction in chiral EFT

- Petschauer et al., "Leading three-baryon force from SU(3) chiral effective filed theory", Phys. Rev. C93, 014001 (2016)
- 2-π exchange ΛNN interaction (a) is first reduced to effective two-body interaction in infinite matter, diagrams (c, d, e), then the contribution to the Λ s.p. potential (c) is estimated. ((d) and (e) are absent for Λ.)
  - Contributions from (d) and (e) diagrams almost cancel each other.
  - Pauli blocking type (c) suppress attraction in free space, which means repulsive effect.

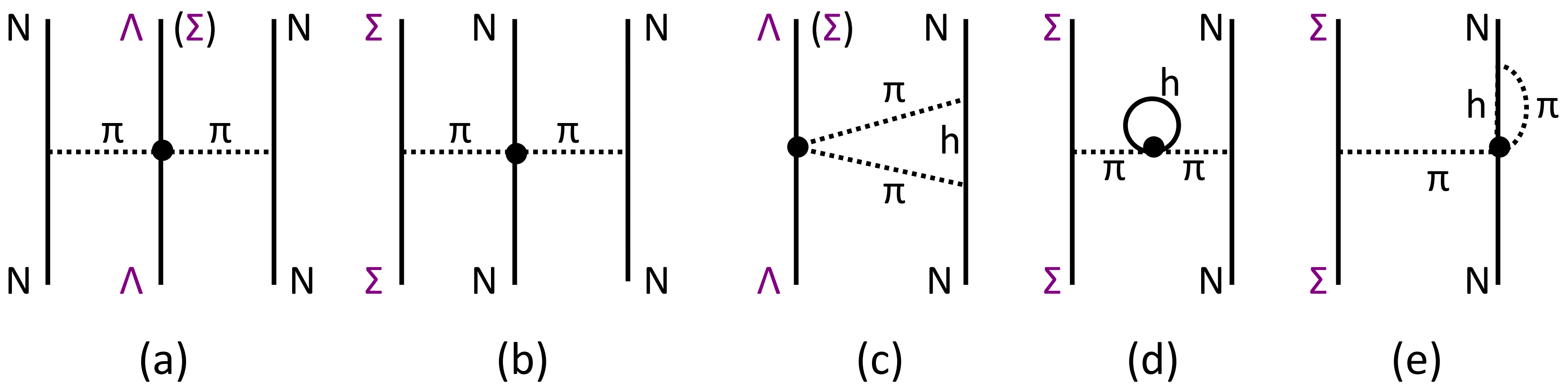

Estimation of 2-π exchange ΛNN contributions to Λ s.p. energies

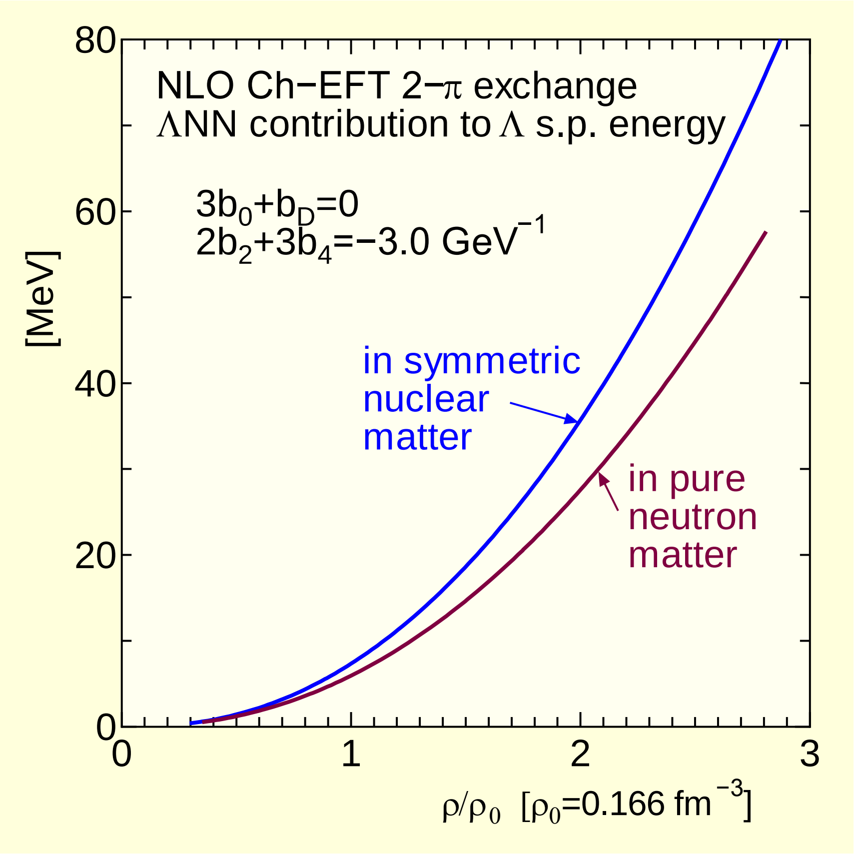

Contributions from contact terms have also to be considered.

$$V_{\Lambda NN} = \frac{g_A^2}{3f_0^4}(\boldsymbol{\tau}_2\cdot\boldsymbol{\tau}_3)\frac{(\boldsymbol{\sigma}_3\cdot\boldsymbol{q}_{63})(\boldsymbol{\sigma}_2\cdot\boldsymbol{q}_{52})}{(\boldsymbol{q}_{63}^2+m_\pi^2)(\boldsymbol{q}_{63}^2+m_\pi^2)} \times\{-(3b_0+b_D)m_\pi^2+(2b_2+3b_4)\boldsymbol{q}_{63}\cdot\boldsymbol{q}_{52}\}$$

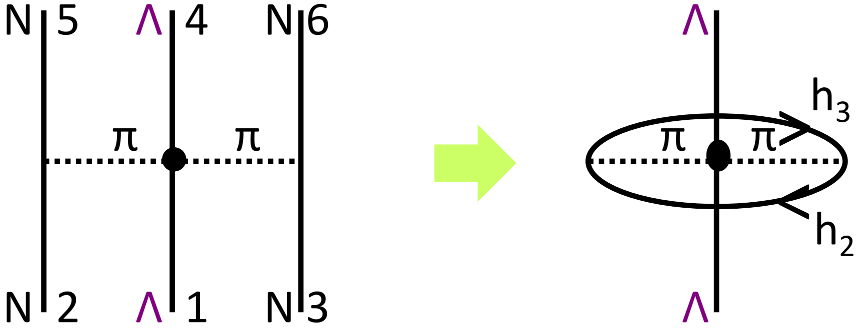

$$U_\Lambda(\boldsymbol{k}_\Lambda) = \frac{1}{2}\sum_{2,3}\langle \boldsymbol{k}_\Lambda\boldsymbol{k}_2\boldsymbol{k}_3|V_{\Lambda NN}|\boldsymbol{k}_\Lambda\boldsymbol{k}_2\boldsymbol{k}_3\rangle_A$$

$$= \frac{g_A^2}{3f_0^4}\frac{1}{(2\pi)^6}\int_0^{k_F} q^2\,dq\,\frac{64\pi^2}{3}(k_F-q)^2 \times(2k_F+q)\frac{4q^2}{(4q^2+m_\pi^2)^2} \times\{-(3b_0+b_D)m_\pi^2+(2b_2+3b_4)q^2\}$$

Appearance of Λ in neutron matter?

- A naive condition for the Λ hyperon to appear in pure neutron matter.

$$U_\Lambda(0) < \frac{\hbar^2}{2m_n} \times {k_{F_n}}^2 + +U_n(k_{F_n})$$

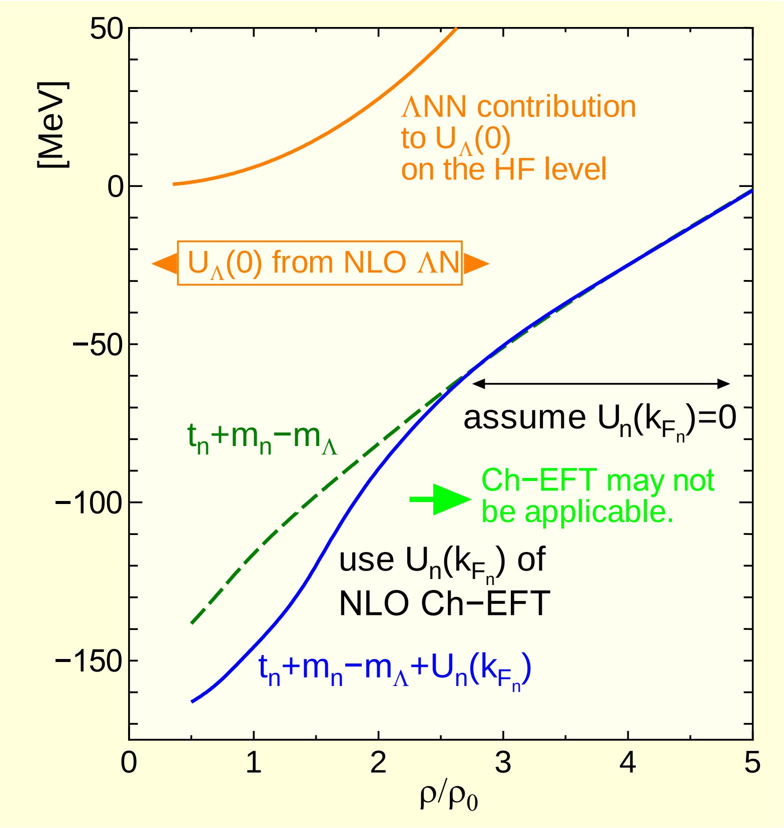

- The NLO YN interactions predict a shallow Λ s.p. potential.
  - $U_\Lambda(0) \cong -20\sim -30$ MeV
- Non-phenomenological YNN interactions have to be considered seriously.
  - Medium modification for the YN interaction, such as Pauli-blocking effects, should exist.
- ΛNN-ΣNN is to be included.

Appearance of Λ in neutron matter?

- A naive condition for the Λ hyperon to appear in pure neutron matter.

$$U_\Lambda(0) < \frac{\hbar^2}{2m_n} \times {k_{F_n}}^2 + +U_n(k_{F_n})$$

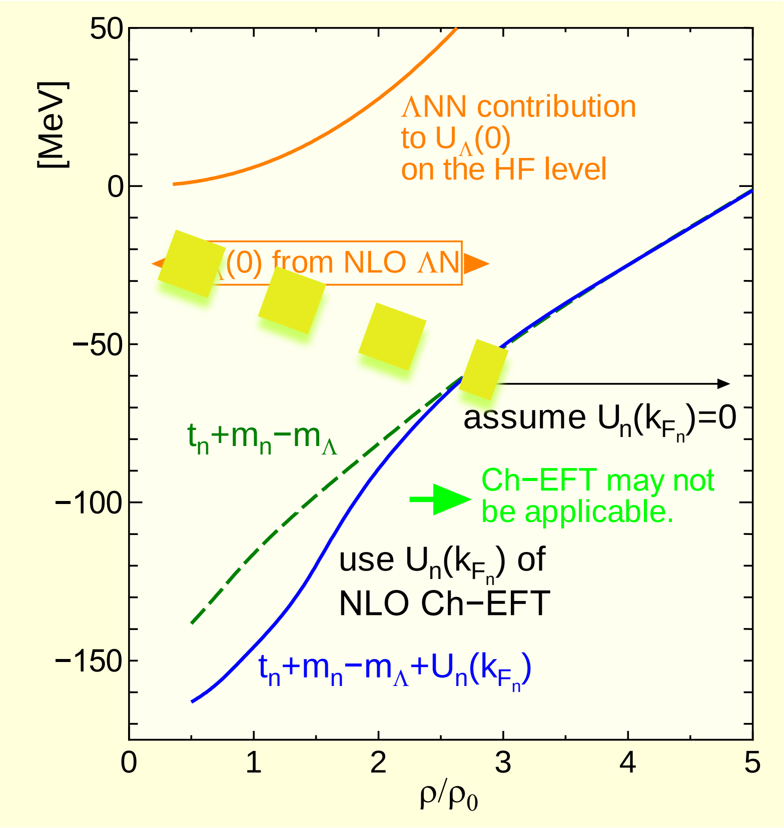

- The NLO YN interactions predict a shallow Λ s.p. potential.
  - $U_\Lambda(0) \cong -20\sim-30$ MeV
- Non-phenomenological YNN interactions have to be considered seriously.
  - Medium modification for the YN interaction, such as Pauli-blocking effects, should exist.
- ΛNN-ΣNN is to be included.

Summary

- Saturation point of N^3LO NN potential in Ch-EFT (as accurate as other modern NN potentials) in nuclear matter is in nuclear matter is naturally on the Coester band.
- Saturation properties are much improved by including 3NFs, which are introduced consistently to the NN sector.
  - In the present calculations, 3NFs are reduced to effective NN forces by folding them over the third nucleon.
- 3NF effects, in addition to the repulsive contribution:
  - Tensor component is enhanced, which brings about some attraction in the $^3S_1$ channel. (and enhance the imaginary potential for the scattering state).
  - Spin-orbit force is enhanced, which is important to account for an empirical strength for shell-structure. (not shown in this talk)
- Using recent NLO YN and YNN interactions, Λ hyperon properties in nuclear matter are calculated.